

DVL Calibration using Data-driven Methods

Zeev Yampolsky* and Itzik Klein

The Hatter Department of Marine Technologies
Charney School of Marine Sciences, University of Haifa
Haifa, Israel

Abstract—Autonomous underwater vehicles (AUVs) are used in a wide range of underwater applications, ranging from seafloor mapping to industrial operations. While underwater, the AUV navigation solution commonly relies on the fusion between inertial sensors and Doppler velocity logs (DVL). To achieve accurate DVL measurements a calibration procedure should be conducted before the mission begins. Model-based calibration approaches include filtering approaches utilizing global navigation satellite system signals. In this paper, we propose an end-to-end deep-learning framework for the calibration procedure. Using stimulative data, we show that our proposed approach outperforms model-based approaches by 35% in accuracy and 80% in the required calibration time.

I. INTRODUCTION

Inertial sensors are used in a wide range of applications, including medical, robotics, and navigation systems [1]. The strapdown inertial navigation system (SINS) utilizes inertial measurements to provide a navigation solution consisting of position, velocity, and orientation. The inertial readings contain noises and other error sources. As a result, the SINS accumulate errors over time, causing the navigation solution to drift [2, 3]. To mitigate such drift, the inertial readings are fused with additional sensors. Although global navigation satellite systems (GNSS) can provide lane-level positioning accuracy [4] the radio signals decay rapidly in water and thus rendering the GNSS unusable underwater [5]. Therefore, the Doppler velocity log (DVL) is commonly used as an additional navigation sensor in autonomous underwater vehicles (AUV) [6, 7].

DVLs are acoustic sensors that transmit acoustic beams to the ocean floor, which in turn, are reflected back. After receiving the beams, the DVL determines each beam’s velocity by employing the Doppler frequency shift effect. Based on the velocity of the beams, the DVL is able to estimate the velocity of the AUV [7, 8]. Thus, by fusing the DVL and SINS measurements, it is possible to minimize the navigation solution error [6, 9].

DVL measurements are also susceptible to error, such as scale factor, bias, misalignment, and zero-mean white Gaussian noise [7, 10–12]. To minimize the error of the DVL measurements and increase the navigation solution accuracy, a calibration process of the DVL is necessary before the mission starts [13, 14].

In most calibration methods, the AUV is required to operate at a predefined trajectory. The majority of works in the literature use GNSS with real-time kinematics (GNSS-RTK), which

can achieve centimeter-level positioning accuracy [15], as a reference unit during the calibration process. Many of these calibration approaches require long and complex calibration trajectories, which in turn require nonlinear estimation filters, making the calibration process complex [16].

Data-driven approaches, have shown great promise in a variety of unrelated areas, such as computer vision and natural language processing [17]. Furthermore, deep learning models have recently been utilized in DVL-related tasks, such as estimating AUV velocity during DVL partial or complete outages [6, 10, 18–20] or in estimating the process noise covariance [21, 22]. Based on the above application of deep-learning models, coupled with their proven usefulness in other domains, a natural question to ask is: can deep-learning approaches shorten calibration time or reduce calibration process complexity? To answer this question, in this work, we derive a DVL calibration approach based on deep-learning methods and GNSS measurements. We show, using stimulative data, that our approach outperforms current model-based approaches for low-end DVLs.

The rest of this paper is organized as follows: Section II discusses the model-based DVL calibration approach. Section III describes our proposed data-driven calibration approach while Section IV describes the calibration results of our proposed approach, compared to a model-based baseline. Lastly, Section V describes the conclusions of this study and our planned future work.

II. PROBLEM FORMULATION

A. GNSS Based DVL Calibration

As a common calibration method, the AUV operates at sea level in shallow waters, allowing it to receive highly accurate GNSS-RTK velocity measurements as a reference while maintaining sufficient depth for the DVL to provide measurements for calibration. Traditionally, GNSS-RTK measurements are related to the DVL measurements using the following error model [13]:

$$\hat{v}^d = (1 + k)\mathbf{R}_b^d(\mathbf{R}_n^b v^n + \omega_{nb}^b \times l_{DVL}) + \delta v^d \quad (1)$$

where \hat{v}^d is the DVL measured velocity expressed in the DVL frame, v^n is the measured GNSS-RTK velocity expressed in the navigation frame, δv^d is a zero-mean white Gaussian noise, k is the scale factor, \mathbf{R}_n^b is the transformation matrix from the navigation frame to the body frame, and \mathbf{R}_b^d is the transformation matrix from the body frame to the DVL frame. The terms ω_{nb}^b and l_{DVL} are the angular velocity of the AUV and the lever-arm between the DVL and center of

*Corresponding author: Z. Yampolsky (email: zyampols@campus.haifa.ac.il).

mass, respectively. The lever arm is generally small and can be precisely measured during installation and compensated for, so the overall term $\omega_{nb}^b \times l_{DVL}$ is generally ignored [12]. For simplicity, and without the loss of generality, we assume \mathbf{R}_b^d to be a known constant transformation matrix. Additionally, assuming the calibration trajectory is a straight line and the calibration period is short, we assume the navigation frame and the body frames coincide, and thus \mathbf{R}_n^b is \mathbf{I}_3 . Thus, (1) reduces to:

$$\hat{\mathbf{v}}^d = (1 + \mathbf{k})\mathbf{R}_b^d \mathbf{v}^n + \delta \mathbf{v}^d \quad (2)$$

Note that (2) is the error model that is most commonly used in the literature, which employs only a scale factor to correct the DVL measurements in relation to the reference measurement. Additionally, in most works in the literature, equal scale factor in all three axes is assumed.

B. Scale Estimation Using Vector Norm

Using the error model presented in (2), the scalar scale factor can be estimated by taking vector modulus on both sides of the equation [11]:

$$\|\hat{\mathbf{v}}^d\| = (1 + k) \|\hat{\mathbf{R}}_b^d \mathbf{v}^n\| \quad (3)$$

Thus, the scale factor k can be determined as follows:

$$\hat{k}_t = \frac{\|\hat{\mathbf{v}}_t^d\|}{\|\hat{\mathbf{R}}_b^d \mathbf{v}_t^n\|} - 1, \quad t = 1, \dots, T \quad (4)$$

where \hat{k} is the estimated scale factor applied to all three axes, $\hat{\mathbf{v}}_t^d$, \mathbf{v}_t^n are the DVL and GNSS-RTK measurements at time step t , and \hat{k}_t is the estimated scale factor at time step t . As a result of estimating the scale factor at each of the T time steps, the average scale factor is:

$$\bar{k} = \frac{1}{T} \sum_{t=1}^T \hat{k}_t \quad (5)$$

Based on this approach, \bar{k} represents the average estimated scale factor at the end of the calibration trajectory.

III. PROPOSED APPROACH

We Propose a data-driven end-to-end approach for estimating the DVL velocity using four different error models as described in Section III-A. Our proposed data-driven approach is a deep neural network (DNN) which consists of two convolution neural networks (CNN) with a fully connected (FC) head. The two CNN are a 1-dimensional CNN (1DCNN) and a 2-dimensional CNN (2DCNN), followed by a FC head. The complete description of the model is provided in Section III-B.

A. DVL Error Models

Combining the error model described in [23] and in (2), it is possible to employ a more general error model:

$$\hat{\mathbf{v}}^d = (1 + \mathbf{k})\hat{\mathbf{R}}_b^d \mathbf{v}^n + \mathbf{b} + \delta \mathbf{v}^d \quad (6)$$

The terms \mathbf{k} and \mathbf{b} refer to the scale factor and bias, respectively. In this work those are defined by:

$$\mathbf{k} = [k_x \ k_y \ k_z]^T \in \mathbb{R}^3 \quad (7)$$

$$\mathbf{b} = [b_x \ b_y \ b_z]^T \in \mathbb{R}^3 \quad (8)$$

where, $k_x \neq k_y \neq k_z$ and $b_x \neq b_y \neq b_z$, that is, we allow different values in each axis. Consequently, we examine four error models in this study:

- 1) **Scale Factor Only:** This model corrects DVL measurements using only a scale factor, as commonly applied in the literature. Two alternatives are presented for the error-models (EM):
 - a) **EM1 - Scalar Scale-Factor:** the scale factor has the same value k in all three axes.
 - b) **EM2 - Vector Scale-Factor:** the scale factor values may differ in each axis as defined in (7).
- 2) **Bias Only:** The bias error model corrects DVL measurements using only constant. There are two alternatives we propose:
 - a) **EM3 - Scalar Bias:** the bias has the same value in all axes.
 - b) **EM4 - Vector Bias:** the bias values may differ in each axis as defined in (8).

The above models, EM1-EM4, are presented in Figure 1.

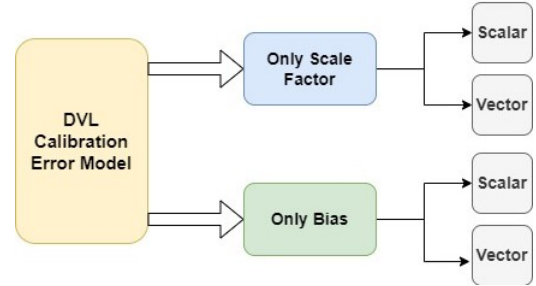


Fig. 1: Four DVL error models examined in this work.

B. Data-Driven Calibration

We offer a multi-head network architecture for the calibration process. It consists of two convolution heads, which differ in the input, its dimension, and kernel dimensions. Following the two CNN heads, the FC head processes the distilled and processed output of the convolution heads in order to estimate the bias vector. The input to the network are the measured velocities of the DVL and GNSS-RTK, denoted as $\tilde{\mathbf{v}}_{DVL}^b$ and $\tilde{\mathbf{v}}_{GNSS}^b$, and referred to as the first input. Within the neural network (NN), the GNSS-RTK velocities vectors are subtracted from the DVL velocities vectors as follows:

$$\tilde{\mathbf{v}}_{sub}^b = \tilde{\mathbf{v}}_{DVL}^b - \tilde{\mathbf{v}}_{GNSS}^b \quad (9)$$

where $\tilde{\mathbf{v}}_{sub}^b$ is considered the second input, even though the subtraction vector is derived directly from the original input, and not considered original data. A block diagram, illustrating the network architecture is presented in Figure 2.

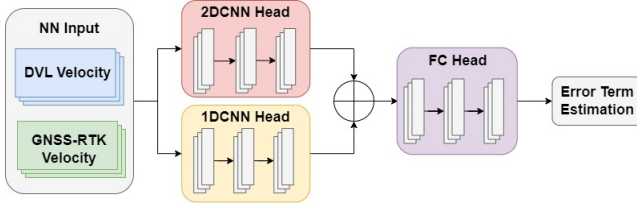


Fig. 2: Block diagram illustration of our architecture. The DVL and GNSS-RTK velocity measurements are fed and processed simultaneously by the two convolution heads, the output is concatenated and fed through the FC head which outputs the estimated DVL error term.

Two separate convolution heads process both inputs simultaneously. The 2DCNN head is fed the first input, the DVL and GNSS-RTK velocities, \tilde{v}_{DVL}^b and \tilde{v}_{GNSS}^b , with an added dimension, so that the data can be treated as a single input of size $1 \times 6 \times n$, where n is the size of time window. The 2DCNN head consists of three 2D convolution layers, each preceded by batch normalization [24] and followed by the activation function Leaky ReLU [25]. A dilated kernel is employed in the first 2D convolution layer by a vertical step of 3, which means that there is a spacing of three between two rows of the kernel points, allowing the layer to process the same axis of both inputs at the same time. The other two 2D convolution layers are not dilated. A dilated first layer is used to replicate the processing of the subtraction vector, \tilde{v}_{sub}^b , by the second 1DCNN head. The 1DCNN head receives as input \tilde{v}_{sub}^b , the subtraction result of the GNSS-RTK from the DVL velocity measurements, and processes it with two 1D convolution layers, none of which is dilated. Both layers are constructed similarly. In both layers, batch normalization is applied first over the input, followed by a 1D convolution layer with a 1D kernel, and then the Leaky ReLU activation function. Both convolution heads outputs are flattened and concatenated. The concatenated data is then fed into the FC head, which consists of 4 FC layers. Each layer has a hyperbolic-tangent (TanH) activation function [26] and dropout with a probability of $p = 0.2$ [27], except for the last layer. The NN learns the dependencies within the input velocities, encodes the data and further processes it whilst feeding it forward down the network layers to output one of the DVL error-models, EM1-EM4, hence minimizing the error between the DVL measurements and the reference GNSS-RTK.

IV. RESULTS

A. Simulation and Data

To examine our proposed approach we created a simulation of a straight-line trajectory where the AUV is travelling at a constant velocity. First, we generate a velocity vector in the body frame, v_{GT}^b , as the simulated ground truth (GT) velocity for the DVL and GNSS-RTK velocity measurements. To simulate DVL velocity measurements, we first rotate, v_{GT}^b , to the DVL frame, v_{GT}^d and then use the DVL's error model as described in [6, 7] to simulate the noisy DVL beams measurements. Then, we project the noisy beams measurements and construct

the DVL measured velocity vector \tilde{v}_{DVL}^d . Lastly, the velocity vector is transformed to body frame \tilde{v}_{DVL}^b . To simulate the GNSS-RTK velocity measurements, $\tilde{v}_{GNSS-RTK}^b$, we add zero-mean white Gaussian noise with a standard deviation, $\sigma_{GNSS-RTK} = 0.005 [\frac{m}{s}]$ to the GT velocity. This pipeline is illustrated in Figure 3.

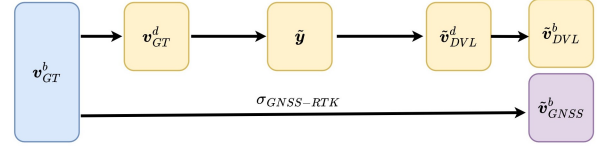


Fig. 3: A simulation pipeline for generating DVL and GNSS measurements.

Two datasets of simulated velocities were created, one for the train set and one for the test set. To simulate the dataset we used the AUV velocity, bias, scale factor, and noise values as defined in Table I. Each train trajectory has a duration of 100 seconds. In total, 7938 trajectories were used in the train dataset according to the parameters and possible combinations between them as defined in Table I. Next, each of the combinations was repeated four times to generate more data. Next, this dataset was divided to train and validation sets using a ratio of 80 : 20%, resulting in a duration of 705.6 and 176.4 hours for the train and validation sets, respectively. Each train and validation trajectory combination was split using a sliding window sized ten seconds and a stride of nine seconds, resulting in eight train and two validation windows for each combination. Considering the number of combinations as described above, produces 254,016 and 63,504 data points for the train and validation datasets, respectively.

TABLE I: AUV and DVL parameter range for creating the training dataset.

	Lower Value	Upper Value	Step size	# Values
X velocity $[\frac{m}{s}]$	1.5	2.1	0.1	7
Scale Factor $[\%]$	0.2	1.5	0.1	14
Bias $[\frac{m}{s}]$	0.001	0.009	0.001	9
Noise $[\frac{m}{s}]$	0.0001	0.001	0.0001	9

In the test set, the same error terms were used to simulate five trajectories, one for the calibration phase and four for the evaluation phase. That is, in the calibration trajectory we apply our proposed NN approach to estimate the DVL error model and apply it on the four evaluation trajectories. We repeat this stage for each error model, EM1-EM4. In creating the test set, GT velocities similar to those in the train set were used, although they were not identical, as presented in Table II. As stated, the first of the five test trajectories is addressed as the calibration trajectory and is 200 seconds long, the other four trajectories are called evaluation trajectories, each is 30 minutes long, resulting in a total of 123 minutes for the test trajectory. To further evaluate our proposed NN approach, we defined four different combinations of error terms, as presented in Table III, denoted as DVL 1 - 4. Thus, in total we have five trajectories for each of the four sets of the DVL errors resulting in a test set duration of 493 minutes.

TABLE II: Velocity vector components used in the calibration and evaluation test trajectories.

	Calib. Traj.	Eval Traj. 1	Eval Traj. 2	Eval Traj. 3	Eval Traj. 4
Velocity X $[\frac{m}{s}]$	2.0	1.8	2.2	1.55	1.9
Velocity Y $[\frac{m}{s}]$	-0.08	0.1	0.5	0.3	-0.05
Velocity Z $[\frac{m}{s}]$	-0.01	0.1	-0.1	-0.08	-0.0084

TABLE III: DVL parameters employed in the test dataset yielding four different types of DVL error models.

	Scale [%]	Bias $[\frac{m}{s}]$	DVL Noise $[\frac{m}{s}]$
DVL 1	0.5	0.001	0.008
DVL 2	0.5	0.001	0.0008
DVL 3	1.0	0.007	0.02
DVL 4	1.0	0.007	0.0002

B. Results

The purpose of this section is to compare the proposed approach with the baseline model-based approach referred to as the "Direct" method. Based on (5), this model-based approach implements the scalar scale estimation approach described in Section II-B. To that end, we employ the root mean square error (RMSE) metric:

$$RMSE(\mathbf{x}_i, \hat{\mathbf{x}}_i) = \sqrt{\frac{\sum_{i=1}^N [\sum_{j=x,y,z} (\mathbf{x}_{i,j} - \hat{\mathbf{x}}_{i,j})^2]}{N}} \quad (10)$$

where \mathbf{x} is the GT velocity vector, $\hat{\mathbf{x}}$ is the corrected DVL velocity by any calibration method, N is the number of measurements, and j represents the XYZ axes. Key point to note is that all the error terms were regressed using the error models presented in Section III-A, but most of them performed equally or worse than the baseline direct approach. Only in regressing the vector bias, EM4, the proposed NN approach managed to compete and produce better results than the baseline approach, thus only EM4 results are presented here.

As a first step, using only the calibration trajectory of the test dataset, a 100 second window is used to estimate the baseline method's scalar scale factor, \hat{k}_{MB} . Based on the estimated scale factor, \hat{k}_{MB} , the remaining 100 seconds velocity vector is calibrated, and the RMSE of the baseline is calculated. To test the convergence time of our proposed NN approach, the same calibration trajectory was divided into five calibration windows of 10, 20, 50, 80, and 100 seconds. The proposed NN approach estimated the error terms for each of the calibration windows. Using the five estimated error terms, the remaining calibration trajectory was corrected and the RMSE was calculated. Therefore, our goal is to examine if our approach achieved lower RMSE compared to the baseline in less than 100 seconds. Table IV presents the results of the convergence time and improvement after averaging the results of 200 Monte Carlo runs. For DVL1-3 our proposed approach requires also 100 seconds to converge, however for DVL4 ours requires only 20 seconds, improving the convergence time by 80%.

By comparing the RMSE of the best-estimated bias vector, $\hat{\mathbf{b}}_{NN}$ with the scalar scale factor, \hat{k}_{MB} of the baseline approach, estimated in the calibration phase on the calibration trajectory, we evaluate the other four evaluation trajectories.

TABLE IV: Convergence to steady-state RMSE

	Baseline Conv. Time [sec]	Ours Conv. Time [sec]	Time Improvement [%]
DVL 4	100	20	80

Table V presents the RMSE results from 200 Monte Carlo runs.

TABLE V: Test set RMSE results comparing between the baseline and our approach.

		Eval Traj. 1	Eval Traj. 2	Eval Traj. 3	Eval Traj. 4	Mean
DVL 1	Baseline	0.024	0.024	0.024	0.024	0.024
	Ours	0.024	0.024	0.024	0.024	0.024
DVL 2	Baseline	0.003	0.003	0.003	0.003	0.003
	Ours	0.005	0.005	0.005	0.004	0.005
DVL 3	Baseline	0.059	0.06	0.06	0.059	0.06
	Ours	0.006	0.061	0.06	0.06	0.06
DVL 4	Baseline	0.007	0.007	0.007	0.007	0.007
	Ours	0.003	0.007	0.006	0.002	0.005

As can be seen in Table V our approach managed to improve only DVL4 by an average of 35%. In practice this means that our approach is suitable only for low-end DVLs.

V. CONCLUSION

In summary, this work investigated the problem of DVL calibration by using GNSS-RTK as a reference. We derived an end-to-end NN framework to reduce the calibration process complexity by using a simplified calibration trajectory and examined different error models, all over simulated data. Our proposed NN approach was able to achieve accurate calibration using a different error term while shortening the calibration time by 80[%]. Additionally, besides shortening the calibration time, our proposed approach was able to improve the RMSE of the baseline method by 35[%] on average. Nevertheless, this major improvement was evident only for DVL4, and not for DVL1-3. It is also important to mention that we presented a generalized error model. By letting the proposed NN regress four different error models, EM1-EM4, we concluded that the proposed approach managed to produce better results only when using EM4. That is, our approach performs well assuming a different bias in each axis and only for low-end DVLs. In our future work, we aim to improve the network performance and evaluate our approach on recorded real-world data.

ACKNOWLEDGEMENT

Z.Y. is supported by the Maurice Hatter Foundation and University of Haifa presidential scholarship for outstanding students on a direct Ph.D. track

REFERENCES

- [1] N. Ahmad, R. A. R. Ghazilla, N. M. Khairi, and V. Kasi, "Reviews on various inertial measurement unit (IMU) sensor applications," *International Journal of Signal Processing Systems*, vol. 1, no. 2, pp. 256–262, 2013.
- [2] Y. Thong, M. Woolfson, J. Crowe, B. Hayes-Gill, and R. Challis, "Dependence of inertial measurements of distance on accelerometer noise," *Measurement Science and Technology*, vol. 13, no. 8, p. 1163, 2002.

- [3] E. Akeila, Z. Salcic, and A. Swain, "Reducing low-cost INS error accumulation in distance estimation using self-resetting," *IEEE Transactions on Instrumentation and Measurement*, vol. 63, no. 1, pp. 177–184, 2013.
- [4] R. Yozevitch, B. Ben-Moshe, and A. Dvir, "GNSS accuracy improvement using rapid shadow transitions," *IEEE Transactions on Intelligent Transportation Systems*, vol. 15, no. 3, pp. 1113–1122, 2014.
- [5] Y. Liu, X. Fan, C. Lv, J. Wu, L. Li, and D. Ding, "An innovative information fusion method with adaptive Kalman filter for integrated INS/GPS navigation of autonomous vehicles," *Mechanical systems and signal processing*, vol. 100, pp. 605–616, 2018.
- [6] N. Cohen and I. Klein, "BeamsNet: A data-driven approach enhancing Doppler velocity log measurements for autonomous underwater vehicle navigation," *Engineering Applications of Artificial Intelligence*, vol. 114, p. 105216, 2022.
- [7] O. Levy and I. Klein, "INS/DVL fusion with DVL based acceleration measurements," *arXiv preprint arXiv:2308.11762*, 2023.
- [8] N. A. Brokloff, "Matrix algorithm for Doppler sonar navigation," in *Proceedings of OCEANS'94*, vol. 3. IEEE, 1994, pp. III–378.
- [9] D. Wang, X. Xu, Y. Yao, T. Zhang, and Y. Zhu, "A novel SINS/DVL tightly integrated navigation method for complex environment," *IEEE Transactions on Instrumentation and Measurement*, vol. 69, no. 7, pp. 5183–5196, 2019.
- [10] N. Cohen, Z. Yampolsky, and I. Klein, "Set-Transformer BeamsNet for AUV velocity forecasting in complete DVL outage scenarios," in *2023 IEEE Underwater Technology (UT)*. IEEE, 2023, pp. 1–6.
- [11] S. Liu, T. Zhang, and Y. Zhu, "A GNSS aided calibration method for DVL error based on the Optimal-REQUEST," *IEEE Sensors Journal*, vol. 22, no. 22, pp. 21 899–21 910, 2022.
- [12] B. Xu, L. Wang, S. Li, and J. Zhang, "A novel calibration method of SINS/DVL integration navigation system based on quaternion," *IEEE Sensors Journal*, vol. 20, no. 16, pp. 9567–9580, 2020.
- [13] B. Xu and Y. Guo, "A novel DVL calibration method based on robust invariant extended Kalman filter," *IEEE Transactions on Vehicular Technology*, vol. 71, no. 9, pp. 9422–9434, 2022.
- [14] D. Wang, X. Xu, Y. Yang, and T. Zhang, "A quasi-newton quaternions calibration method for DVL error aided GNSS," *IEEE Transactions on Vehicular Technology*, vol. 70, no. 3, pp. 2465–2477, 2021.
- [15] T. Li, H. Zhang, Z. Gao, Q. Chen, and X. Niu, "High-accuracy positioning in urban environments using single-frequency multi-GNSS RTK/MEMS-IMU integration," *Remote sensing*, vol. 10, no. 2, p. 205, 2018.
- [16] Z. Ning, X. Pan, and W. Wu, "Research on fast calibration and moving base alignment of SINS/DVL integrated navigation system," *IEEE Sensors Journal*, 2023.
- [17] I. Klein, "Data-driven meets navigation: Concepts, models, and experimental validation," in *2022 DGON Inertial Sensors and Systems (ISS)*. IEEE, 2022, pp. 1–21.
- [18] M. Yona and I. Klein, "Compensating for partial Doppler velocity log outages by using deep-learning approaches," in *2021 IEEE International Symposium on Robotic and Sensors Environments (ROSE)*. IEEE, 2021, pp. 1–5.
- [19] —, "MissBeamNet: Learning missing Doppler velocity log beam measurements," *arXiv preprint arXiv:2301.11597*, 2023.
- [20] Y. Yao, X. Xu, X. Xu, and I. Klein, "Virtual beam aided SINS/DVL tightly coupled integration method with partial vc measurements," *IEEE Transactions on Vehicular Technology*, vol. 72, no. 1, pp. 418–427, 2022.
- [21] B. Or and I. Klein, "ProNet: Adaptive process noise estimation for INS/DVL fusion," in *2023 IEEE Underwater Technology (UT)*. IEEE, 2023, pp. 1–5.
- [22] N. Cohen and I. Klein, "A-KIT: Adaptive Kalman-informed transformer," 2024.
- [23] P. Liu, S. Zhao, L. Qing, Y. Ma, B. Lu, and D. Hou, "A calibration method for DVL measurement errors based on observability analysis," in *2019 Chinese Control Conference (CCC)*. IEEE, 2019, pp. 3851–3856.
- [24] S. Ioffe and C. Szegedy, "Batch normalization: Accelerating deep network training by reducing internal covariate shift," in *International conference on machine learning*. pmlr, 2015, pp. 448–456.
- [25] B. Xu, N. Wang, T. Chen, and M. Li, "Empirical evaluation of rectified activations in convolutional network," *arXiv preprint arXiv:1505.00853*, 2015.
- [26] S. R. Dubey, S. K. Singh, and B. B. Chaudhuri, "Activation functions in deep learning: A comprehensive survey and benchmark," *Neurocomputing*, 2022.
- [27] N. Srivastava, G. Hinton, A. Krizhevsky, I. Sutskever, and R. Salakhutdinov, "Dropout: a simple way to prevent neural networks from overfitting," *The journal of machine learning research*, vol. 15, no. 1, pp. 1929–1958, 2014.